Tian Lide (Orcid ID: 0000-0002-8866-7744)
Jiang Wei (Orcid ID: 0000-0002-6355-7637)
Lu Zheng-Tian (Orcid ID: 0000-0002-1887-0018)

^{81}Kr dating of the Guliya ice cap, Tibetan Plateau

Lide Tian[1,2,3,4*], Florian Ritterbusch[5], Ji−Qiang Gu[5], Shui-Ming Hu[5], Wei Jiang[5], Zheng-Tian Lu[5*], Di Wang [1], Guo-Min Yang[5]

[1]Institute of International Rivers and Eco-security, Yunnan University, Kunming 650500, China.

[2]CAS Center for Excellence in Tibetan Plateau Earth Sciences, Chinese Academy of Sciences, Beijing 100101, China.

[3]College of Resource and Environment, University of Chinese Academy of Sciences, Beijing, 100190, China

[4]Yunnan Key Laboratory of International Rivers and Transboundary Eco–security, Yunnan University, Kunming 650091, China

[5]Hefei National Laboratory for Physical Sciences at the Microscale, CAS Center for Excellence in Quantum Information and Quantum Physics, University of Science and Technology of China, Hefei 230026, China

Corresponding authors:

Lide Tian (ldtian@ynu.edu.cn) , Zheng-Tian Lu (ztlu@ustc.edu.cn)

Key Points:

- Radiometric ^{81}Kr dating of bottom ice from the Guliya ice cap
- ^{81}Kr data yield upper age limits in the range of 15-74 ka
- ^{81}Kr results difficult to reconcile with ages previously obtained for the Guliya ice core based on ^{36}Cl and δ^{18}O

This article has been accepted for publication and undergone full peer review but has not been through the copyediting, typesetting, pagination and proofreading process which may lead to differences between this version and the Version of Record. Please cite this article as doi: 10.1029/2019GL082464

Abstract

We present radiometric ^{81}Kr dating results for ice samples collected at the outlets of the Guliya ice cap in the western Kunlun Mountains of the Tibetan Plateau. This first application of ^{81}Kr dating on mid-latitude glacier ice was made possible by recent advances in Atom Trap Trace Analysis, particularly a reduction in the required sample size down to 1 µLSTP of krypton. Eight ice blocks were sampled from the bottom of the glacier at three different sites along the southern edges. The ^{81}Kr data yield upper age limits in the range of 15-74 ka (90% confidence level). This is an order of magnitude lower than the ages exceeding 500 ka which the previous ^{36}Cl data suggest for the bottom of the Guliya ice core. It is also significantly lower than the widely used chronology up to 110 ka established for the upper part of the core based on ice δ^{18}O.

Keywords： ^{81}K dating; Guliya ice cap; ice core chronology; Tibetan Plateau;

Plain Language Summary

The oldest ice that has ever been found outside of the polar regions is from the bottom of the Guliya ice cap in the western Kunlun mountains on the Tibetan Plateau. Previous dating results from the Guliya ice core, drilled in 1992, indicate that the bottom ice is more than 500 thousand years old. However, due to the lack of alternative dating methods in that time range, the age scale of the Guliya ice core has so far not been checked independently.

In this work we present dating results for the Guliya ice cap with a new dating method for ice based on the radioactive decay of the extremely rare krypton isotope ^{81}Kr. Eight ice samples were retrieved at three different margin sites of the Guliya ice cap, where the old bottom ice is expected to resurface. The ^{81}Kr measurements for these samples yield upper age limits in the range of 15-74 ka, which is significantly lower than the previous dating results for the ice core.

1 Introduction

Alpine ice cores in the mid- and low-latitude regions provide high-resolution records of past climate and environment. High rates of ice accumulation and melting are responsible for the relatively short history of ice core records on the Tibetan Plateau as compared to the polar regions. Longer ice cores and older ice are being sought on the Tibetan Plateau for the purpose of extending the climate history in this region. The Malan and Puruogangri ice cores in the central Tibetan Plateau [*Thompson et al.*, 2006; *Wang et al.*, 2003] and the Dasuopu ice core in the middle of the Himalayas [*Thompson et al.*, 2000; *Yao et al.*, 2002] provide records of the past several thousand years. Samples from the bottom of the Dunde ice core in the northeastern Tibetan Plateau were first interpreted to be glacial-stage ice [*Thompson et al.*, 1989], but later proved to be a Holocene deposit [*Thompson et al.*, 2005]. The longest (308.6 m) ice core and the oldest bedrock ice so far discovered on the Tibetan Plateau is from the Guliya ice cap in the western Kunlun Mountains [*Yao et al*. 1997, *Thompson et al*. 1997]. Developing a chronology for this Guliya ice core (GIC1992 hereafter), as for Tibetan ice cores in general, is challenging. Dating by layer counting is difficult for ice cores from the Tibetan Plateau because the monsoonal type precipitation pattern in this region generates weaker seasonal variation [*Hou et al.*, 2003]. For GIC1992 an age scale up to 110 ka was established down to 266 m depth by comparing the $\delta^{18}O$ signal with the CH_4 record from GISP2 in Greenland. Moreover, the ^{36}Cl data suggest that the bottom ice may be older than 500 ka. Since then, the GIC1992 record has been widely used as a reference for correlating regional climate signals [*e.g. Cheng et al.*, 2012; *Chevalier et al.*, 2011; *Cosford et al.*, 2008; *Hayashi et al.*, 2017; *Mahowald et al.*, 2011].

However, the established Guliya chronology is difficult to reconcile with several recent findings. *Cheng et al.* [2012] encountered inconsistencies between the $\delta^{18}O$ record of GIC1992 and the Kesang stalagmite record. Their work suggests that the relationship between $\delta^{18}O$ and CH_4 may be inversed, leading to a shortening of the GIC1992 age scale by a factor of two. Meanwhile, at the Chongce ice cap (~30 km away from the GIC1992 drilling site), luminescence dating provides an upper age limit of 42±4 ka for the basal sediment [*Zhang et al.*, 2018], which is an order of magnitude lower than what the ^{36}Cl data suggests for the bottom ice of GIC1992. Moreover, ^{14}C dating in combination with ice flow modeling for ice cores

from the Chongce ice cap indicates Holocene deposition [*Hou et al.*, 2018], which is consistent with all other Tibetan ice cores except GIC1992. Given the proximity between the Guliya and the Chongce ice cap, these results make it difficult to argue that the large difference in age scale between GIC1992 and the other Tibetan ice cores is due to different local climate conditions in the western Kunlun Mountains [*Thompson et al.*, 2005]. All the foregoing findings raise the need for examining the GIC1992 chronology with an independent dating method.

^{81}Kr is a cosmogenic radionuclide with a half-life of 229 ± 11 ka. The ^{81}Kr concentration in the atmosphere (isotopic abundance ^{81}Kr /Kr ~1×10^{-12}) is spatially homogeneous with only small changes over the past 1.5 million years [*Buizert et al.*, 2014]. These properties as well as its chemical inertness make it a desirable tracer for groundwater and ice over the age range of 40 ka to 1.3 Ma [*Loosli and Oeschger*, 1969; *Lu et al.*, 2014]. Meanwhile, the anthropogenic ^{85}Kr (half-life 10.76 ± 0.02 a), which is mainly produced by nuclear fuel reprocessing, can be used to identify any young (< 60 a) components or contamination of an old sample with modern air [*Winger et al.*, 2005]. Development of the analytical method of Atom Trap Trace Analysis (ATTA) has made radiokrypton dating available to the earth science community at large [*Jiang et al.*, 2012]. Due to the large required sample size (5-10 μL STP of krypton), so far ^{81}Kr has been used mainly for dating groundwater while for glacier ice only a demonstration study was conducted on large blue ice samples (~ 350 kg) from Taylor Glacier, Antarctica [*Buizert et al.*, 2014]. Recently, the required sample size for ^{81}Kr- and ^{85}Kr-analysis has been reduced down to 1 μL STP of krypton, which can be extracted from about 10 kg of Antarctic ice (containing ~100 mL STP air per kg ice) or 20 – 40 kg of Tibetan glacier ice (25 - 50 mL STP air/kg) [*Li et al.*, 2011]. This sample size is still too large to re-assess the historic GIC1992 directly, but is sufficient for ^{81}Kr dating of samples from the margin sites of the Guliya ice cap, as presented in this work.

2 Methods

2.1 Site description and ice sampling

Guliya is a large ice cap in the western Kunlun Mountains on the Tibetan Plateau with a total area of about 376 km^2 [*Thompson et al.*, 1997; *Yao et al.*, 1997]. Its southern part is of nonsurge

type with stationary terminus positions [*Yasuda and Furuya*, 2015]. Remote sensing data show that the glaciers in this region have experienced less change in recent decades compared to other glaciated mountainous regions in western China [*Shangguan et al.*, 2017]. The Guliya ice cap even gained mass from 2000-2015 [*Kutuzov et al.*, 2018] primarily due to increasing precipitation in the westerly regime [*Yao et al.*, 2012]. Ice core drilling and ground penetrating radar show that the glacier thickness varies from about 50 m at the summit to a maximum thickness of 371 m at a location 1.5 km upstream of the GIC1992 drilling site (Fig. 1) [*Kutuzov et al.*, 2018; *Thompson et al.*, 1997]. The glacier flows from the summit at 6710 m altitude down to the margins at approximately 5500 m [*Thompson et al.*, 1997] with an average slope of < 3 -5° [*Kutuzov et al.*, 2018]. Limited field observation indicates increasing negative surface mass balance going from the equilibrium line altitude of around 6000 m to lower elevation sites [*Li et al.*, 2019]. The ablation of the ice cap is also characterized by cliff melting at the end of the glacier outlets so that the bottom ice layers become accessible over large sections of the glacier edge.

The criteria used in selecting sampling sites include less crevasse in the upper-stream ice flow and exposure of basal ice. The samples were collected at the bases of the vertical ice walls at three glacier outlets between 2015 and 2017. GLY1 is located downstream of the GIC1992 drilling site from 1992 [*Thompson et al.*, 1997]; GLY2 and GLY3 are located at the outlets of the glacier summit (Fig. 1). In total eight ice blocks were sampled, of which four were retrieved from a 6 m deep cave (hereafter cave samples) to avoid potential gas loss and contamination with modern air due to ice fractures [*Craig et al.*, 1990; *Buizert et al.*, 2014]. As the ^{85}Kr results demonstrated that this practice is unnecessary at these sites, the later four ice samples were retrieved near the surface of the ice wall (hereafter surface samples).

At GLY1 (Fig. 1), a 6 meter deep horizontal cave was dug using a chainsaw and a pick along a clear bubble ice layer near the bottom of the ice wall. The underlying 2 m section contains dust layers with dark mud and pebbles and is thus not suitable for sampling with a chainsaw. Two vertically adjacent ice block samples (GLY1-1 on top of GLY1-2) were collected in the white bubble layer at the end of the cave. At GLY2, also a 6 m deep ice cave was dug approximately 3 m above the bottom dust layer, and two ice blocks were collected in the bubble ice layer.

Moreover, two near-surface glacier ice samples were retrieved along the ice cliff in order to compare dating results between cave and surface ice as well as to date the silty ice at the very bottom. At GLY3, silty ice blocks from the very bottom were collected (Fig. 2).

In addition to the samples for radiokrypton dating, ice samples for stable water isotope analysis were collected along the bottom of the ice wall surface. The surface layers were removed in the field since they may have been affected by melting. A glacier ice column with a total length of more than 5.3 m was sampled to the visible lowermost part of the glacier cliff at GLY2. A 1.27 m long ice column was sampled at GLY3 in the same layer where the ice blocks for ^{81}Kr analysis had been sampled (Fig. 2). All the ice samples were kept in a freezer at -20℃ during the transport to the city of Lhasa, where they were stored in a cold room until degassing or cutting. The ice samples for δ^{18}O analysis from GLY1 were lost due to technical failure of the cooling facility such that only the δ^{18}O profiles from GLY2 and GLY3 are presented in the following.

2.2 Air extraction from the ice samples

For ^{81}Kr and ^{85}Kr analysis, the air trapped in the ice has to be extracted. Prior to extraction, the surface of the ice samples is cleaned to remove any layers or flaky debris that may contain modern air. The ice is then brought out of the cold room and placed in a stainless steel chamber which is thereafter sealed and evacuated for about 30 min by scroll pumps through a water trap (stainless steel bellow immersed in ethanol at -80 ^{o}C). Since during pumping the chamber is constantly being flushed by the water vapor from the sublimating ice, the remaining atmospheric gas in the container is rendered negligible. After evacuation, the chamber is heated by a stove for 60 - 90 min (depending on the ice mass) until the ice has completely melted. The gas released from the ice passes through the water trap and is compressed into a sample cylinder. The air content of the ice sample is determined based on the final pressure in the sample cylinder (Table 1). Extraction efficiencies higher than 95% and contamination with modern air below 1% are typically achieved with this degassing method at a processing time of about 2-3 hours per sample. More details on the extraction system and procedure are provided in the supporting material.

2.3 Krypton purification and ^{81}Kr measurement

The extracted gas from the ice samples was sent to the University of Science and Technology of China (USTC) for krypton purification and for ATTA analysis of both ^{81}Kr and ^{85}Kr. Krypton is separated from the extracted gas using a purification system based on titanium gettering and gas chromatography [*Tu et al.*, 2014], typically yielding krypton purities and recoveries both higher than 90%.

The ^{81}Kr and ^{85}Kr measurements are performed with the latest ATTA instrument at USTC, where individual ^{81}Kr and ^{85}Kr atoms are selectively laser-cooled and then detected in a magneto-optical trap. The stable and abundant ^{83}Kr is also measured for normalization. The resulting ^{81}Kr/^{83}Kr and ^{85}Kr/^{83}Kr ratios for the sample are compared to the corresponding ratios of a reference krypton gas to derive the ^{81}Kr abundance as a percentage of the atmospheric value (pMKr) and the ^{85}Kr abundance given in the units of dpm/cc (decay per minutes per cc STP krypton), a convention originating from decay counting. More details on ^{81}Kr and ^{85}Kr analysis with ATTA can be found in *Jiang et al* [2012].

2.4 Stable water isotopes

The ice columns collected along the ice cliff at GLY2 and GLY3 were cut in the cold room into samples of 2 cm intervals. The melted ice samples were measured using Picarro L2140i liquid water analyzer in the Institute of International River and Eco-security, Yunnan University, with a precision of ±0.15‰ for δ^{18}O referenced to VSMOW2.

3 Results and discussion

3.1 δ^{18}O results

Figure 2 shows the oxygen isotope variation along the 5.3 m bottom ice at GLY2 and the 1.27 m profile at GLY3. It is difficult to match these short δ^{18}O profiles from GLY2 and GLY3 with the δ^{18}O record from GIC1992 [*Thompson et al.*, 1997]. However, the δ^{18}O fluctuations along the profile provide hints whether the ice originates from the bottom or not. The accumulation layers of the glacier rapidly become thinner towards the bottom. The fast fluctuations of the δ^{18}O signal is averaged out when the thickness of the layers become less than the 2 cm cutting

interval. The large fluctuations in the $\delta^{18}O$ profile at GLY3 as well as in the upper part of GLY2 are comparable to those at the top of GIC1992 [*Thompson et al.*, 2018], suggesting that these samples are not derived from the bottom of the glacier. The samples were collected from the visible lowest part of the glacier cliff, which is not necessarily the lowest part of the ice as the bottom may be covered by debris from the glacier. This explanation is supported by the observation of a large amount of pebbles being deposited in front of the glacier cliff at GLY3. In contrast, the fluctuations in the $\delta^{18}O$ profile at GLY2 exhibit reduced fluctuations towards the bottom of the glacier. This indicates that GLY2-4, collected at the bottom of the GLY2 profile, is likely close to the very bottom of the glacier ice. The reduced fluctuations in the lower 3.3 m of the $\delta^{18}O$ profile at GLY2 may also result from mixing of ice of different ages due to complex flow leading to averaging of the $\delta^{18}O$ values. The same mechanism may be responsible for the higher fluctuations in the $\delta^{18}O$ profile at GLY3 and at the top of GLY2 (e.g. if layers with higher $\delta^{18}O$ values are transported next to layers with lower $\delta^{18}O$ values) although no stratigraphic disturbance has been observed at the three sampling sites.

It is difficult to match the $\delta^{18}O$ records from this study to the one from GIC1992 because of the high ambiguity in matching the excursions and because the ice at GLY2 and GLY3 originates from a different accumulation zone than the ice at the GIC1992 drilling site. At the height of 3.3 m the $\delta^{18}O$ record at GLY2 exhibits a shift in the mean from -17.5‰ to -15‰ and below that the standard deviation is reduced from 2‰ to 1.1‰ (figure 2). This behavior is similar for the $\delta^{18}O$ signal of GIC1992 with the difference that the mean $\delta^{18}O$ value at the bottom 40 m is higher than the bottom 3.3 m at GLY2 by about 2‰. This is likely due to the altitude difference of the accumulation zones of the ice at GLY2 and GIC1992.

3.2 Air content

The measured air contents in the ice samples are listed in Table 1. They vary from 32 mL STP/kg to 59 mL STP/kg, which is typical for Himalayan ice cores [*Hou et al.*, 2007; *Li et al.*, 2011] and significantly lower than the air content of Antarctic ice, typically ranging between 100 - 120 mL STP/kg [*Buizert et al.*, 2014*; Raynaud and Lebel*, 1979], or that of Greenland ice

at 80 - 100 mL/kg [*Raynaud et al.*, 1997]. This is due to the lower air pressure at high elevation (5500-6700 m) of the deposition site and the higher temperature compared to Antarctica [*Eicher et al.*, 2016; *Martinerie et al.*, 1992]. We deliberately collected the samples from ice layers with visibly high bubble content and avoided those with transparent ice which are likely layers of re-frozen meltwater.

3.3 ^{85}Kr and ^{81}Kr results

The measured ^{81}Kr and ^{85}Kr abundances for the eight glacier ice samples as well as two air samples of Lhasa are listed in Table 1. As described above, the ^{85}Kr in the atmosphere has almost exclusively been produced anthropogenically in the past 60 years. Therefore, any sample older than that should have a vanishing ^{85}Kr abundance. Five of the eight samples have ^{85}Kr activity levels below 3% of the Lhasa air value (Table 1), whereas GLY2-1, GLY2-2 and GLY3-2 have ^{85}Kr values corresponding to about 8%, 3% and 5%, respectively. Air leaks are thoroughly investigated on instruments used in the degassing, purification and ATTA measurement, leading to the conclusion that contamination of modern air during these processes is below 1%. It thus seems more likely that modern air had already entered the ice prior to sampling, e.g. by cracking/melting and refreezing, as has been observed in earlier works on glacier ice close to the surface of margin sites [*Craig et al.*, 1990; *Buizert et al.*, 2014]. Since there is no obvious correlation between ^{85}Kr and whether the sample is from the surface or from a cave, potential contamination processes at the very front of the glacier ice cliff do not seem to be responsible for that.

Since the measured ^{81}Kr abundances are close to the modern value of 100 pMKr, contamination of modern air at these low concentrations does not affect the reported ^{81}Kr abundances within the given precisions. For all samples they are consistent with modern atmospheric ^{81}Kr abundance within 1σ, except for GLY3-1 which still lies within a 2σ error. We translate the measured relative ^{81}Kr abundances into ^{81}Kr-ages using the Feldman-Cousins method [*Feldman and Cousins*, 1998]. As the ^{81}Kr abundances are close to modern, this method yields upper age limits (90% confidence level) for the individual samples that range between 15-74 ka.

3.4 Implication for the Guliya ice core chronology

The obtained results for ^{81}Kr and δ^{18}O of the Guliya margin samples allow for a discussion in the context of the results from GIC1992 [*Thompson et al.,* 1997] (see introduction). The ^{81}Kr measurements do not show evidence for ice older than 74 ka at the bottom of the sampled margin sites of the Guliya ice cap. For the samples from GLY1, where the ice from GIC1992 is expected to outcrop [*Kutuzov et al.,* 2018], the upper limits for the ^{81}Kr age do not exceed 52 ka. For GLY2-4, whose δ^{18}O profile exhibits bottom ice characteristics, the ^{81}Kr results provide an upper age limit of only 25 ka. The obtained upper age limits do not necessarily rule out the existence of older ice somewhere else in the Guliya ice cap. It is possible that the old ice at the bottom of GIC1992 is frozen to the bedrock and does not flow out to the margin sites. However, radar measurements indicate that the ice at the bottom of GIC1992 does flow and is not trapped at the bedrock [*Kutuzov et al.,* 2018]. A further explanation is that the stratigraphy of the glacier ice is folded when travelling from the GIC1992 drilling site to the margin, such that the old ice may not be at the bottom. No evidence for folding was observed at the glacier terminals, which exhibit clear horizontal layer structures, but folding on intermediate distance scales may have occurred. Yet another possibility is that the bottom 100 m of GIC1992, which are supposedly older than 50 ka, are rapidly thinning towards the outlet of the glacier, and therefore may be contained in a much smaller vertical extent at the very bottom of the glacier cliff. Since the samples at GLY1 were taken in about 2 m height above bedrock, they may not reach into this old bottom section. However, measurements of the mass balance and the glacier surface velocity [*Thompson et al.,* 1995; *Li et al.,* 2019; *Chadwell*, 2017] indicate that a large fraction of the upper glacier layers is lost when flowing from the equilibrium line altitude to the edge of the glacier at GLY1 where the remaining glacier cliff is about 10 m in height. Therefore, it does not seem likely that the bottom 100 m at the GIC1992 drilling site are thinning to below our sampling height about 2 m above bedrock at GLY1.

4 Conclusions and Outlook

Radiometric ^{81}Kr dating has been used to determine the age of bottom ice samples at the Guliya ice cap. Eight ice blocks, each weighing 28-69 kg, were collected at three different outlets of the glacier, and analyzed for ^{81}Kr using the Atom Trap Trace Analysis method. The ^{81}Kr results yield upper limits in the range of 15-74 ka, which is an order of magnitude lower than previously suggested by ^{36}Cl dating of the Guliya ice core and also significantly lower than the Guliya chronology reaching up to 110 ka based on δ^{18}O measurements. After results from the Kesang stalagmite cave (~ 860 km distance to the Guliya ice cap) and the Chongce ice cap (~ 30 km distance), the ^{81}Kr data in this work (obtained directly from bottom samples of the Guliya ice cap) represent yet another result that calls for further dating measurements to check the established Guliya chronology. Measurements of ^{14}C, ^{36}Cl, ^{10}Be, $\delta^{18}O_{atm}$ and argon isotope ratios are planned for a new Guliya ice core that has been drilled in 2015 close to the location of the 1992 Guliya core drilling site [*Thompson et al.*, 2018]. Meanwhile, at the USTC laboratory, work is in progress to further reduce the sample size required for ^{81}Kr analysis so that bottom samples from the Guliya ice core can be measured directly.

Acknowledgments

We thank the two anonymous reviewers for their valuable comments and suggestions. This work is funded by National Natural Science Foundation of China (41530748), the National Key Research and Development Program of China (2016YFA0302200) and the Chinese Academy of Sciences (XDB21010200). We thank Lili Shao and Cheng Wang from the Institute of Tibetan Plateau Research for their assistance in the ice degassing and Lei Zhao from USTC for purifying the krypton samples. Stable water isotopes data are available in the supporting information.

References

Buizert, C., et al. (2014), Radiometric ^{81}Kr dating identifies 120,000-year-old ice at Taylor Glacier, Antarctica, Proceedings of the National Academy of Sciences of the United States of America, 111(19), 6876-6881, doi: 10.1073/pnas.1320329111.

Chadwell, C. (2017), Reliability analysis for design of stake networks to measure glacier surface velocity, Journal of Glaciology, 45(149), 154-164, doi: 10.1017/s0022143000003130.

Cheng, H., P. Z. Zhang, C. Spötl, R. L. Edwards, Y. J. Cai, D. Z. Zhang, W. C. Sang, M. Tan, and Z. S. An (2012), The climatic cyclicity in semiarid-arid central Asia over the past 500,000 years, Geophysical Research Letters, 39(1), doi: 10.1029/2011gl050202.

Chevalier, M.-L., G. Hilley, P. Tapponnier, J. Van Der Woerd, J. Liu-Zeng, R. C. Finkel, F. J. Ryerson, H. Li, and X. Liu (2011), Constraints on the late Quaternary glaciations in Tibet from cosmogenic exposure ages of moraine surfaces, Quaternary Science Reviews, 30(5), 528-554, doi: https://doi.org/10.1016/j.quascirev.2010.11.005.

Cosford, J., H. Qing, D. Yuan, M. Zhang, C. Holmden, W. Patterson, and C. Hai (2008), Millennial-scale variability in the Asian monsoon: Evidence from oxygen isotope records from stalagmites in southeastern China, Palaeogeography, Palaeoclimatology, Palaeoecology, 266(1), 3-12, doi: https://doi.org/10.1016/j.palaeo.2008.03.029.

Craig, H., T. E. Cerling , R. D. Willis, W. A. Davis, C. Joyner, N. Thonnard (1990), Krypton-81 in Antarctic ice: first measurement of a Krypton age on ancient ice. EOS 71:1825.

Eicher, O., M. Baumgartner, A. Schilt, J. Schmitt, J. Schwander, T. F. Stocker, and H. Fischer (2016), Climatic and insolation control on the high-resolution total air content in the NGRIP ice core, Climate of the Past, 12(10), 1979-1993, doi: 10.5194/cp-12-1979-2016.

Feldman, G.J. and R.D. Cousins (1998), Unified approach to the classical statistical analysis of small signals, Physical Review D, 57, 3873–3889, doi: 10.1103/PhysRevD.57.3873

Hayashi, T., et al. (2017), Ecological variations in diatom assemblages in the Paleo-Kathmandu Lake linked with global and Indian monsoon climate changes for the last 600,000 years, Quaternary Research, 72(3), 377-387, doi: 10.1016/j.yqres.2009.07.003.

Hou, S., D. Qin, J. Jouzel, V. Masson-Delmotte, U. Von Grafenstein, A. Landais, N. Caillon, and J. Chappellaz (2004), Age of Himalayan bottom ice cores, Journal of Glaciology, 50(170), 467-468, doi: 10.3189/172756504781829981.

Hou, S., J. Chappellaz, J. Jouzel, P. C. Chu, V. Masson-Delmotte, D. Qin, D. Raynaud, P. A. Mayewski, V. Y. Lipenkov, and S. Kang (2007), Summer temperature trend over the past two millennia using air content in Himalayan ice, Climate of the Past, 3(1), 89-95, doi: 10.5194/cp-3-89-2007

Hou, S., T. M. Jenk, W. Zhang, C. Wang, S. Wu, Y. Wang, H. Pang, and M. Schwikowski (2018), Age ranges of the Tibetan ice cores with emphasis on the Chongce ice cores, western Kunlun Mountains, The Cryosphere, 12(7), 2341-2348, doi: 10.5194/tc-12-2341-2018.

Jiang, W., et al. (2012), An atom counter for measuring ^{81}Kr and ^{85}Kr in environmental samples, Geochimica et Cosmochimica Acta, 91, 1-6, doi: 10.1016/j.gca.2012.05.019.

Kutuzov, S., L. G. Thompson, I. Lavrentiev, and L. Tian (2018), Ice thickness measurements of Guliya ice cap, western Kunlun Mountains (Tibetan Plateau), China, Journal of Glaciology, 1-13, doi: 10.1017/jog.2018.91.

Li, J., B. Xu, and J. Chappellaz (2011), Variations of air content in Dasuopu ice core from AD 1570–1927 and implications form climate change, Quaternary International, 236(1-2), 91-95, doi: 10.1016/j.quaint.2010.05.026.

Li, S., T. Yao, W. Yu, W. Yang, and M. Zhu (2019), Energy and mass balance characteristics of the Guliya ice cap in the West Kunlun Mountains, Tibetan Plateau, Cold Regions Science and Technology, 159, 71-85, doi: 10.1016/j.coldregions.2018.12.001.

Loosli, H. H., and H. Oeschger (1969), ^{37}Ar and ^{81}Kr in the atmosphere, Earth and Planetary

Science Letters, 7(1), 67-71, doi: 10.1016/0012-821X(69)90014-4.

Lu, Z. T., et al. (2014), Tracer applications of noble gas radionuclides in the geosciences, Earth-Science Reviews, 138, 196-214, doi: 10.1016/j.earscirev.2013.09.002.

Mahowald, N., S. Albani, S. Engelstaedter, G. Winckler, and M. Goman (2011) Model insight into glacial–interglacial paleodust records, Quaternary Science Reviews, 30(7-8), 832-854, doi: 10.1016/j.quascirev.2010.09.007.

Martinerie, P., D. Raynaud, D. M. Etheridge, J.-M. Barnola, and D. Mazaudier (1992), Physical and climatic parameters which influence the air content in polar ice, Earth and Planetary Science Letters, 112(1), 1-13, doi: 10.1016/0012-821X(92)90002-D.

Raynaud, D., and B. Lebel (1979), Total gas content and surface elevation of polar ice sheets, Nature, 281(5729), 289-291, doi: 10.1038/281289a0.

Raynaud, D., J. Chappellaz, C. Ritz, and P. Martinerie (1997), Air content along the Greenland Ice Core Project core: A record of surface climatic parameters and elevation in central Greenland, Journal of Geophysical Research: Oceans, 102(C12), 26607-26613, doi:10.1029/97JC01908.

Shangguan, D., S. Liu, Y. Ding, J. Li, Y. Zhang, L. Ding, X. Wang, C. Xie, and G. Li (2017), Glacier changes in the west Kunlun Shan from 1970 to 2001 derived from Landsat TM/ETM+ and Chinese glacier inventory data, Annals of Glaciology, 46(1), 204-208, doi: 10.3189/172756407782871693.

Thompson, L. G., T. Yao, E. Mosley-Thompson, M. E. Davis, K. A. Henderson, and P. Lin (2000), A high-resolution millennial record of the south Asian monsoon from Himalayan ice cores, Science, 289(5486), 1916-1920, doi: 10.1126/science.289.5486.1916.

Thompson, L. G., M. E. Davis, E. Mosley-Thompson, P. N. Lin, K. A. Henderson, and T. A. Mashiotta (2005), Tropical ice core records: evidence for asynchronous glaciation on Milankovitch timescales, Journal of Quaternary Science, 20(7-8), 723-733, doi: 10.1002/jqs.972.

Thompson, L. G., E. Mosley-Thompson, M. E. Davis, T. A. Mashiotta, K. A. Henderson, P. N. Lin, and T. Yao (2006), Ice core evidence for asynchronous glaciation on the

Tibetan Plateau, Quaternary International, 154(0), 3-10, doi: 10.1016/j.quaint.2006.02.001.

Thompson, L. G., E. Mosley-Thompson, M. E. Davis, J. F. Bolzan, J. Dai, L. Klein, T. Yao, X. Wu, Z. Xie, and N. Gundestrup (1989), Holocene--late Pleistocene climatic ice core records from Qinghai-Tibetan plateau, Science, 246(4929), 474-477, doi: 10.1126/science.246.4929.474.

Thompson, L. G., T. Yao, M. E. Davis, K. A. Henderson, E. Mosley-Thompson, P. N. Lin, J. Beer, H. A. Synal, J. ColeDai, and J. F. Bolzan (1997), Tropical climate instability: The last glacial cycle from a Qinghai-Tibetan ice core, Science, 276(5320), 1821-1825, doi: 10.1126/science.276.5320.1821.

Thompson, L. G., et al. (2018), Ice core records of climate variability on the Third Pole with emphasis on the Guliya ice cap, western Kunlun Mountains, Quaternary Science Reviews, 188, 1-14, doi: 10.1016/j.quascirev.2018.03.003.

Tu, L.-Y., G.-M. Yang, C.-F. Cheng, G.-L. Liu, X.-Y. Zhang, and S.-M. Hu (2014), Analysis of Krypton-85 and Krypton-81 in a Few Liters of Air, Analytical Chemistry, 86(8), 4002-4007, doi: 10.1021/ac500415a.

Wang, N., L. G. Thompson, M. E. Davis, E. Mosley-Thompson, T. Yao, and J. Pu (2003), Influence of variations in NAO and SO on air temperature over the northern Tibetan Plateau as recorded by $\delta^{18}O$ in the Malan ice core, Geophysical Research Letters, 30(22), CLM 1-5, doi: 10.1029/2003gl018188.

Winger, K., J. Feichter, M. B. Kalinowski, H. Sartorius, and C. Schlosser (2005), A new compilation of the atmospheric Krypton-85 inventories from 1945 to 2000 and its evaluation in a global transport model, Journal of Environmental Radioactivity, 80(2), 183-215, doi: 10.1016/j.jenvrad.2004.09.005.

Yao, T., L. G. Thompson, and Y. Shi (1997), Climatic variation since the Last Interglacial recorded in the Guliya ice core, Science in China (D), 40(6), 662-668, doi: 10.1007/BF02877697.

Yao, T., et al. (2012), Different glacier status with atmospheric circulations in Tibetan Plateau and surroundings, Nature Climate Change, 2(9), 663-667, doi: 10.1038/Nclimate1580.

Yao, T., K. Duan, B. Xu, N. Wang, J. Pu, S. Kang, X. Qin, and L. G. Thompson (2002), Temperature and methane changes over the past 1000 years recorded in Dasuopu glacier (central Himalaya) ice core, Annals of Glaciology, Vol 35, 35, 379-383.

Yasuda, T., and M. Furuya (2015), Dynamics of surge-type glaciers in West Kunlun Shan, Northwestern Tibet, Journal of Geophysical Research: Earth Surface, 120(11), 2393-2405, doi: 10.1002/2015jf003511.

Zhang, Z., S. Hou, and S. Yi (2018), The first luminescence dating of Tibetan glacier basal sediment, The Cryosphere, 12(1), 163-168, doi: 10.5194/tc-12-163-2018.

Table 1. Compilation of the ^{81}Kr and ^{85}Kr results. The ^{81}Kr abundance is reported in units of pMKr (percent Modern Krypton). The atmospheric level is 100 pMKr. The ^{85}Kr abundance is reported in the units of dpm/cc (decays per minute per cc STP of krypton). The errors are 1σ standard deviations whereas upper limits are reported for a 90% confidence level.

Sample	Note	Weight kg	Air content mL STP/kg	Krypton µL STP	^{85}Kr dpm /cc	^{81}Kr pMKr	^{81}Kr age ka
GLY1-1	Cave	34	52	1.4	< 1.5	97 ± 7	< 52
GLY1-2	Cave	28	46	1.3	1.6 ± 0.2	106 ± 6	< 15
GLY2-1	Cave	53	37	1.1	6.1 ±1.8	93 ±7	< 74
GLY2-2	Cave	69	41	2.5	2.5 ±0.2	97 ± 5	< 39
GLY2-3	Surface	52	45	1.7	0.7 ± 0.2	97 ± 5	< 39
GLY2-4	Surface	30	32	0.7	< 0.4	104 ± 7	< 25
GLY3-1	Surface	43	29	1.8	1.0 ± 0.2	93 ± 5	< 58
GLY3-2	Surface	36	50	1.4	4.1 ± 0.4	98 ± 6	< 45
Lhasa-Air1	May 2017	-	-	0.9	75 ± 2	-	-
Lhasa-Air2	Oct 2017	-	-	0.9	76 ± 3	-	-

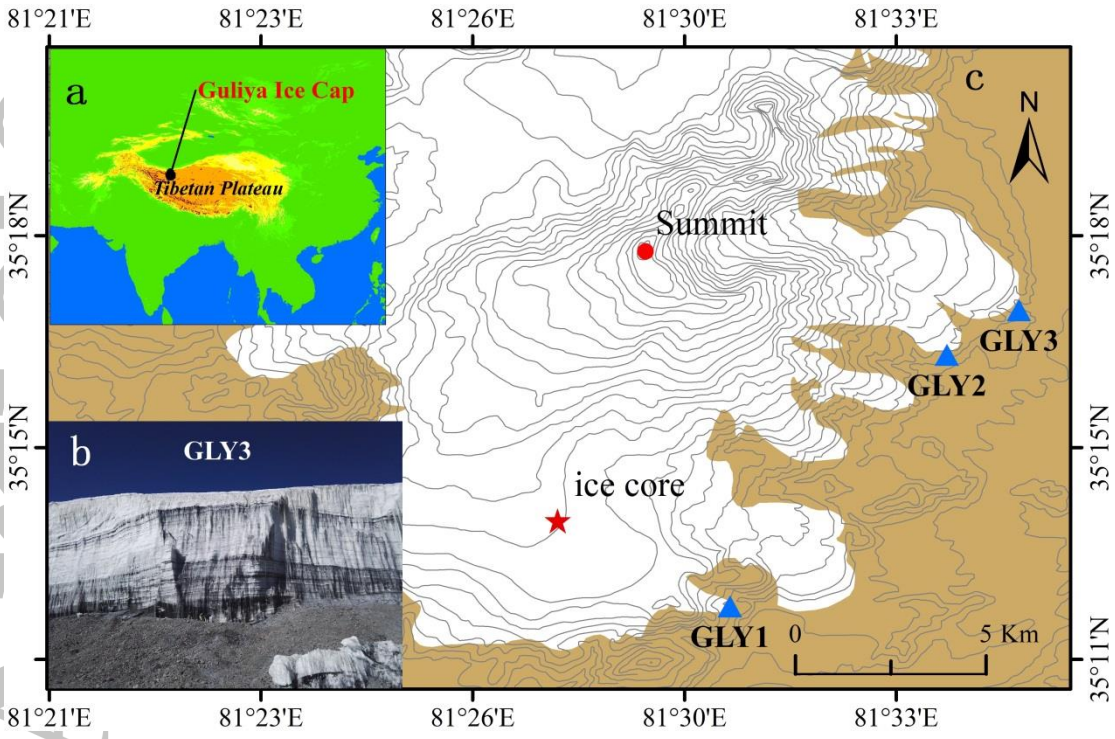

Figure 1. (a) Location of the Guliya ice cap on the Tibetan Plateau ; (b) photograph showing the glacier cliff (~20 m tall) at sampling site GLY3; (c) Sampling sites GLY1, GLY2 and GLY3 for bottom ice of the Guliya ice cap during 2015-2017. The red dot marks the summit (6710 m a.s.l.) and the red star the location of the Guliya ice core (GIC1992) drilling site (6200 m a.s.l.) from 1992 [*Thompson et al.*, 1997].

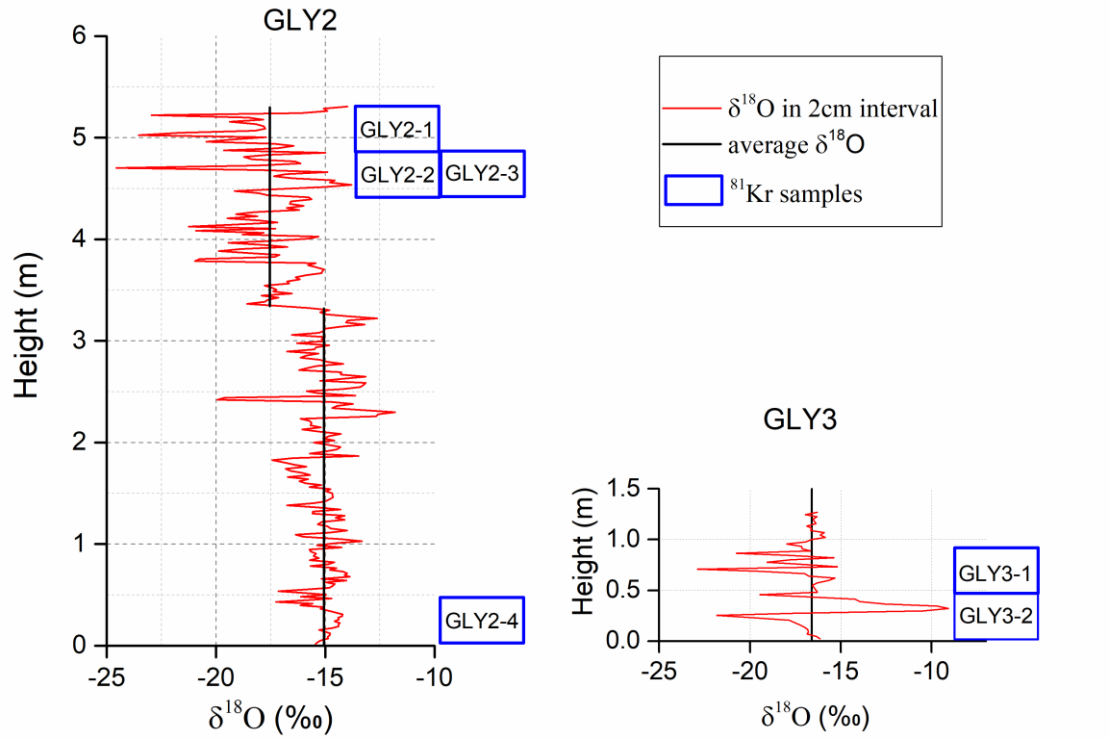

Figure 2. Vertical $\delta^{18}O$ profiles along a 5.3 m column at GLY2 and a 1.27 m column at GLY3. The boxes show the positions of the ^{81}Kr-dated glacier ice samples along the vertical profiles. The zero in height corresponds to the visible bottom of the glacier cliff, but is not necessarily the bedrock as debris may cover the lowermost part of the glacier. The size and the vertical position of the samples are roughly to scale. For GLY2, the $\delta^{18}O$ data of the lower 3.3 m have an average of -15.0‰ and a standard deviation (std) of 1.1‰ whereas in the upper 2 m the average is -17.5‰ (std=2.0‰). For GLY3, the average is -16.6‰ (std=2.4‰).